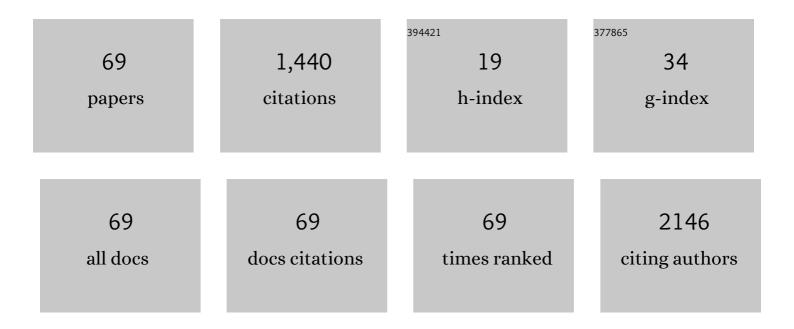
## **Dongsheng Tang**

List of Publications by Year in descending order

Source: https://exaly.com/author-pdf/7566290/publications.pdf Version: 2024-02-01



#	Article	IF	CITATIONS
1	Graphitic Carbon Nitride with Dopant Induced Charge Localization for Enhanced Photoreduction of CO <sub>2</sub> to CH <sub>4</sub> . Advanced Science, 2019, 6, 1900796.	11.2	251
2	Highly Robust Nonâ€Noble Alkaline Hydrogenâ€Evolving Electrocatalyst from Seâ€Doped Molybdenum Disulfide Particles on Interwoven CoSe <sub>2</sub> Nanowire Arrays. Small, 2020, 16, e1906629.	10.0	70
3	Metallic MoO <sub>2</sub> â€Modified Graphitic Carbon Nitride Boosting Photocatalytic CO <sub>2</sub> Reduction via Schottky Junction. Solar Rrl, 2020, 4, 1900416.	5.8	59
4	Engineering Inâ€Plane Nickel Phosphide Heterointerfaces with Interfacial sp HP Hybridization for Highly Efficient and Durable Hydrogen Evolution at 2 A cm <sup>â^'2</sup> . Small, 2022, 18, e2105642.	10.0	57
5	Effect of H2O adsorption on the electrical transport properties of double-walled carbon nanotubes. Carbon, 2006, 44, 2155-2159.	10.3	51
6	Broad spectral response photodetector based on individual tin-doped CdS nanowire. AIP Advances, 2014, 4, .	1.3	47
7	Simultaneous Triplet Exciton–Phonon and Exciton–Photon Photoluminescence in the Individual Weak Confinement CsPbBr <sub>3</sub> Micro/Nanowires. Journal of Physical Chemistry C, 2019, 123, 25349-25358.	3.1	47
8	Boosting Alkaline Hydrogen and Oxygen Evolution Kinetic Process of Tungsten Disulfideâ€Based Heterostructures by Multiâ€ <b>s</b> ite Engineering. Small, 2022, 18, e2104624.	10.0	44
9	Memristive properties of hexagonal WO3 nanowires induced by oxygen vacancy migration. Nanoscale Research Letters, 2013, 8, 50.	5.7	38
10	Ultrathin MoO2 nanosheets with good thermal stability and high conductivity. AIP Advances, 2017, 7, .	1.3	37
11	Structure and Photoluminescence of Pure and Indium-Doped ZnTe Microstructures. Journal of Physical Chemistry C, 2011, 115, 1415-1421.	3.1	33
12	Tinâ€Assisted Sb <sub>2</sub> S <sub>3</sub> Nanoparticles Uniformly Grafted on Graphene Effectively Improves Sodiumâ€ion Storage Performance. ChemElectroChem, 2018, 5, 811-816.	3.4	33
13	Ultrathin GaGeTe p-type transistors. Applied Physics Letters, 2017, 111, .	3.3	28
14	In-Plane Anisotropic Raman Response and Electrical Conductivity with Robust Electron–Photon and Electron–Phonon Interactions of Air Stable MoO <sub>2</sub> Nanosheets. Journal of Physical Chemistry Letters, 2019, 10, 2182-2190.	4.6	28
15	Multi-layered MoS <sub>2</sub> phototransistors as high performance photovoltaic cells and self-powered photodetectors. RSC Advances, 2015, 5, 45239-45248.	3.6	27
16	Luminescence and local photonic confinement of single ZnSe:Mn nanostructure and the shape dependent lasing behavior. Nanotechnology, 2013, 24, 055201.	2.6	24
17	Anomalous Temperature-Dependent Raman Scattering of Vapor-Deposited Two-Dimensional Bi Thin Films. Journal of Physical Chemistry C, 2018, 122, 24459-24466.	3.1	22
18	Near-infrared radiation absorption properties of covellite (CuS) using first-principles calculations. AIP Advances, 2016, 6, .	1.3	21

Dongsheng Tang

#	Article	IF	CITATIONS
19	Modulating memristive performance of hexagonal WO3 nanowire by water-oxidized hydrogen ion implantation. Scientific Reports, 2016, 6, 32712.	3.3	21
20	Synthesis and photoluminescence of pure and Mn doped CdS nanowires. Physica E: Low-Dimensional Systems and Nanostructures, 2013, 47, 162-166.	2.7	19
21	Temperature-Dependent Raman Scattering of Large Size Hexagonal Bi2Se3 Single-Crystal Nanoplates. Applied Sciences (Switzerland), 2018, 8, 1794.	2.5	19
22	TiO2 Nanosheet Arrays with Layered SnS2 and CoOx Nanoparticles for Efficient Photoelectrochemical Water Splitting. Nanoscale Research Letters, 2019, 14, 342.	5.7	18
23	Fabrication of SnO2 one-dimensional nanosturctures with graded diameters by chemical vapor deposition method. Journal of Crystal Growth, 2010, 312, 220-225.	1.5	17
24	Reconfigurable resistive switching devices based on individual tungsten trioxide nanowires. AIP Advances, 2013, 3, .	1.3	17
25	Ultrahigh sensitivity and gain white light photodetector based on GaTe/Sn : CdS nanoflake/nanowire heterostructures. Nanotechnology, 2014, 25, 445202.	2.6	17
26	Surface polarons and optical micro-cavity modulated broad range multi-mode emission of Te-doped CdS nanowires. Nanotechnology, 2018, 29, 465709.	2.6	17
27	Raman investigation of layered ZrGeTe4 semiconductor. Applied Physics Letters, 2019, 114, .	3.3	17
28	Ultrafast hydrogen-ion storage in MoO3 nanoribbons. Solid State Ionics, 2020, 353, 115380.	2.7	17
29	1D ZnSSeâ€ZnSe Axial Heterostructure and its Application for Photodetectors. Advanced Electronic Materials, 2019, 5, 1800770.	5.1	16
30	Amorphous Co–Pi anchored on CdSe/TiO2 nanowire arrays for efficient photoelectrochemical hydrogen production. Journal of Materials Science, 2019, 54, 3284-3293.	3.7	16
31	Solar radiation shielding properties of transparent LaB6 filters through experimental and first-principles calculation methods. Ceramics International, 2016, 42, 14278-14281.	4.8	15
32	High-performance photodetectors based on bandgap engineered novel layer GaSe <sub>0.5</sub> Te <sub>0.5</sub> nanoflakes. RSC Advances, 2016, 6, 60862-60868.	3.6	15
33	Branched TiO <sub>2</sub> Nanorod Arrays Decorated with Au Nanostructure for Plasmon-Enhanced Photoelectrochemical Water Splitting. Journal of the Electrochemical Society, 2020, 167, 026509.	2.9	15
34	Experimental observation of radial breathing-like mode of graphene nanoribbons. Applied Physics Letters, 2012, 100, .	3.3	14
35	First-principles prediction of solar radiation shielding performance for transparent windows of GdB6. Journal of Applied Physics, 2016, 119, .	2.5	14
36	Resistive switching behavior of hexagonal sodium tungsten bronze nanowire. Solid State Ionics, 2017, 308, 107-111.	2.7	14

Dongsheng Tang

#	Article	IF	CITATIONS
37	Single crystalline SmB6 nanowires for self-powered, broadband photodetectors covering mid-infrared. Applied Physics Letters, 2018, 112, .	3.3	14
38	Cs0.33WO3 as a high-performance transparent solar radiation shielding material for windows. Journal of Applied Physics, 2018, 124, .	2.5	14
39	Positive and Negative Photoconductivity Conversion Induced by H2O Molecule Adsorption in WO3 Nanowire. Nanoscale Research Letters, 2019, 14, 144.	5.7	14
40	Structure and optical properties of pure and doped ZnO 1D nanostructures. Materials Letters, 2013, 91, 369-371.	2.6	13
41	Controlled Fabrication of Intermolecular Junctions of Singleâ€Walled Carbon Nanotube/Graphene Nanoribbon. Small, 2013, 9, 2405-2409.	10.0	13
42	The effect of dopant and optical micro-cavity on the photoluminescence of Mn-doped ZnSe nanobelts. Nanoscale Research Letters, 2013, 8, 314.	5.7	12
43	Enhanced memristive performance of individual hexagonal tungsten trioxide nanowires by water adsorption based on Grotthuss mechanism. Materials Research Express, 2014, 1, 025025.	1.6	12
44	Scanning tunneling microscopy image modeling for zigzag-edge graphene nanoribbons. Applied Physics Letters, 2011, 98, 263103.	3.3	11
45	Large-scale synthesis and electrical transport properties of single-crystalline SmB <sub>6</sub> nanowires. Journal Physics D: Applied Physics, 2016, 49, 265302.	2.8	11
46	Electrical characterization of H2S adsorption on hexagonal WO3 nanowire at room temperature. Journal of Applied Physics, 2014, 116, 164310.	2.5	10
47	Tuning emission property of CdS nanowires via indium doping. Journal of Alloys and Compounds, 2013, 551, 150-154.	5.5	9
48	Spin-polarized surface state transport in a topological Kondo insulator SmB6 nanowire. Physical Review B, 2017, 95, .	3.2	9
49	High-performance near-infrared photodetector based on quasi one-dimensional layered (TaSe4)2I. Applied Physics Letters, 2021, 119, .	3.3	8
50	Large physisorption strain and edge modification of Pd on monolayer graphene. Nanoscale, 2013, 5, 124-127.	5.6	7
51	Temperature dependent Raman of BiTe nanotubes. AIP Advances, 2018, 8, .	1.3	7
52	Spatial distribution of spin polarization in a channel on the surface of a topological insulator. Journal of Physics Condensed Matter, 2012, 24, 185301.	1.8	6
53	Magnetic control of valley and spin degrees of freedom via magnetotransport in <i>n</i> -type monolayer MoS <sub>2</sub> . Journal of Physics Condensed Matter, 2014, 26, 485008.	1.8	6
54	Effect of oxygen vacancies on the resistive switching behavior of hexagonal WO <sub>3</sub> nanowire. Materials Research Express, 2019, 6, 085072.	1.6	6

DONGSHENG TANG

#	Article	IF	CITATIONS
55	Effect of an oxidizing environment on the phase structure of lead oxide nanowires. AIP Advances, 2013, 3, 022120.	1.3	5
56	Effect of hydrogen ions in the adsorbed water layer on the resistive switching properties of hexagonal WO3 nanowire. Journal of Applied Physics, 2019, 126, 054303.	2.5	5
57	Directly Probing Interfacial Coupling in a Monolayer MoSe <sub>2</sub> and CuPc Heterostructure. ACS Applied Materials & Interfaces, 2021, 13, 18372-18379.	8.0	5
58	Controllable fully spin-polarized transport in a ferromagnetically doped topological insulator junction. Journal of Applied Physics, 2014, 115, 154310.	2.5	4
59	Large-scale synthesis and quantitative characterization of size-controllable potassium tungsten bronze nanowires. Journal Physics D: Applied Physics, 2018, 51, 095305.	2.8	4
60	Surface polarity induced three-dimensional wurtzite ZnS/ZnSxSe1â°'x nano-heterostructures with integrating emission property. CrystEngComm, 2013, 15, 9988.	2.6	3
61	Strong temperature-strain coupling in the interface of Sb thin film on flexible PDMS substrate. Applied Physics Letters, 2019, 115, .	3.3	3
62	In-plane anisotropic Raman response of layered In2Te5 semiconductor. Applied Physics Letters, 2021, 118, 182105.	3.3	3
63	Interplay between topological surface states and superconductivity in SmB6/NbN tunnel junctions. Physical Review B, 2017, 96, .	3.2	3
64	Optimization of hydrogen-ion storage performance of tungsten trioxide nanowires by niobium doping. Nanotechnology, 2022, 33, 105403.	2.6	3
65	Stable green and red dual-color emission in all-inorganic halide-mixed perovskite single microsheets. RSC Advances, 2020, 10, 18368-18376.	3.6	2
66	Photoluminescence and Boosting Electron–Phonon Coupling in CdS Nanowires with Variable Sn(IV) Dopant Concentration. Nanoscale Research Letters, 2021, 16, 19.	5.7	2
67	Multi-Stable Conductance States in Metallic Double-Walled Carbon Nanotubes. Nanoscale Research Letters, 2009, 4, 538-543.	5.7	1
68	Wide spectrum multi-sub-band modulation of excitons and defect state emission simultaneously in surface oxidized CdS micro/nano-wires. AIP Advances, 2020, 10, 125213.	1.3	0
69	Emission enhancement and exciton species modulation in monolayer WS <sub>2</sub> via decoration of CdTe quantum dots. Applied Physics Letters, 2022, 120, 261105.	3.3	О